

Fracture of Fibrous Metal Matrix Composites

GEORGE J. DVORAK and YEHIA A. BAHEI-EL-DIN
*Department of Civil Engineering, Rensselaer Polytechnic Institute,
Troy, New York 12180-3590, USA*

1. INTRODUCTION

Fracture of fibrous metal matrix composites is not well understood. Most of the available information on the subject has been derived from several experimental studies in which fracture strength was measured on notched specimens of different geometries [1-6]. The significant conclusion was that standard or modified fracture mechanics approaches could not be used to predict the onset of fracture from a preexisting notch in a unidirectional B-Al composite. Previous efforts to model the fracture process focused on determination of local stresses in the unbroken fibers ahead of the notch [7]. These efforts have been often hindered by lack of understanding of the elastic-plastic behavior of the composite. While it was well known that possibly extensive plastic deformation at the notch tip preceded fracture, the relevant deformation fields could not be analyzed by continuum mechanics methods. Recent progress in development of the plasticity theory of composite materials and of its experimental verification makes such an analysis feasible in fibrous systems.

A brief outline of fracture analysis of unidirectional composites is presented in this paper. The first part describes the results of an experimental study of the deformation field and of fracture strength measurements on unidirectional B-Al plate specimens. The second part presents a numerical study in which the plasticity theory of composites was employed to facilitate analysis of plastic deformation in notched specimens before fracture. The results show that the deformation field is dominated by shear deformation in discrete plastic zones at the notch tip. A comparison of the numerical results with experiments indicates that the onset of fracture in the B-Al system is controlled by a critical magnitude of local fracture strain in a certain representative volume ahead of the notch.

2. EXPERIMENTAL WORK

The material used in the experimental program was six-ply 6061 Al/B, unidirectionally reinforced at 50% by volume. Ten 25.4 mm and seven 50.8 mm wide specimens were cut with a diamond saw. The specimens were 305 mm long with the fiber in the longitudinal direction. A center notch was cut in each specimen, in the direction perpendicular to the fibers, using the

electrostatic discharge machining technique. These notches were 0.2 mm wide. The free length of each specimen between grips was 203 mm. All specimens were tested in the as-fabricated condition. For reference purposes, three unnotched specimens were also tested for evaluation of ultimate strength (1659 MPa), and axial elastic modulus (235.63 GPa).

Table 1 shows specimen dimensions and fracture strength results for the notched B-A λ specimens. The failure load P_{ult} , overall ultimate stresses at failure σ_{ult} , and net ligament stresses at failure σ_{lig} are given for each specimen. Also, averages denoted by top bars, of the last two stresses for each group of specimens of the same size are shown. These data were compared with results found by other investigators [1-6] from tests performed on as-fabricated unidirectional 6061 Al/B specimens with a center notch. Figure 1 shows the results for tests on 25.4mm wide specimens, and Fig. 2 for tests on 50.8mm wide specimens. The data shown in Figs. 1 and 2 fall into rather narrow bands. That suggests that on the relative strength scale the available experimental data can be regarded as a single set. Therefore, one should be able to derive predictions of the relative strength reduction in notched specimens from a single model of the fracture process.

Table 1

Results of fracture tests on center-notched B/A λ specimens

Specimen #	W (mm)	2c/W	P _{ult} (kN)	σ_{ult} (MPa)	σ_{lig} (MPa)	$\bar{\sigma}_{ult}$ (MPa)	$\bar{\sigma}_{lig}$ (MPa)	R _o (mm)
A1	25.7	0.4	17.60	642	1061	636	1070	14.38
A2	24.4	0.4	16.40	630	1079			
A3	25.2	0.6	10.68	396	1005	425	1059	16.81
A4	25.6	0.6	12.40	454	1113			
A5	25.3	0.7	8.70	322	1103	315	1071	16.07
A6	25.4	0.7	8.94	329	1108			
A7	25.5	0.7	8.02	295	1003	859	1075	
A8	25.4	0.2	23.82	883	1109			
A9	25.4	0.2	23.35	863	1079	295	986	
A10	25.4	0.2	22.57	831	1037			
B1	50.8	0.3	31.75	586	840	602	862	16.08
B2	50.8	0.3	33.55	618	884			
B3	50.6	0.5	24.56	455	915	456	917	18.63
B4	50.5	0.5	24.55	456	919			
B5	50.9	0.7	15.95	294	987	295	986	19.94
B6	50.8	0.7	16.42	302	1007			
B7	50.9	0.7	15.63	288	963			

Growth of the discrete plastic shear zones which form at the notch tips in the direction parallel to the fibers was monitored by a fine bar code which was photodeposited prior to testing on one face of each specimen following the procedure suggested by Costin et al. [8]. The direction of the deposited bar code lines was perpendicular to the fiber direction which, of course, coincided with the direction of the discrete plastic zones. As these zones developed under increasing load, the bar code deformed and revealed the essential features of their geometry. In particular, the width of the zone, the relative displacement across the zone, and

the width average of the local shear strain in the zone were evaluated from observed distortions of the bar code which were photographed at about ten load levels in each test.

Four similar plastic zones formed in each specimen during loading, two at each notch tip. An example appears in Fig. 3 which shows the distorted pattern found at 0.977 of ultimate load on specimen B1. Results of actual measurements performed on the distorted bar code have shown that the observed zone widths were equal to about 0.25 to 0.5 mm at the notch tip and to about 1 to 2 mm at the end of the observable distortions of the bar pattern. At these extremes, the measured vertical displacements across the zone were equal to about 0.025 mm and 0.1 mm, respectively. Accordingly, the measured shear strains in the zones were of the order of 0.1 to 0.01. The lower magnitude suggests the limit of sensitivity of the bar code method. In comparison, the initial yield strain of the composite in shear was equal to about 0.001. Accordingly, the bar code technique enabled us to detect experimentally only part (R_o) of the total length R of the zone. Selected values of measured zone length R_o appear in Table 1.

Figure 4 shows a photograph of the broken specimen B1 which appeared at 0.977 of ultimate load in Fig. 3. Long splits were often found in the discrete plastic zones at failure. They are clearly visible on the photograph, and as such they serve as convenient markers of the notch size. Their length, however, is much smaller than the total zone length. Examination of the bar code lines on the broken specimens revealed no trace of bar code distortion along the fracture surface. This suggests that the fracture process was not self-similar, the plastic zones formed only before failure, but not during final fracture.

3. FRACTURE STRENGTH PREDICTIONS

One of the important results of the experimental work is the detection of the long discrete plastic zones in the notched specimens before fracture, and the finding that such zones do not form during fracture. These observations can be utilized to facilitate calculation of the stress field in notched composites and prediction of their fracture strength. In principle, the stress field in the center notched specimens can be determined as shown in Fig. 5 where the specimen geometry has been modified to reflect the existence of the zones. Taken together, the original notch and the zones form an H crack. A constant shear stress τ^* , equal to the longitudinal shear flow stress of the composite, is applied in the zones to reflect the effect of the local plastic deformation on the adjacent elastic material. The total ligament stress σ_T in the plane of the notch can be found as a sum of the uniform stress $\sigma_{lig} = \bar{\sigma}/(1-2c/W)$ caused by the applied overall stress $\bar{\sigma}$, and of the stress $\Delta\sigma$ induced by the shear stresses τ^* applied to the ligament boundary by the plastic zones.

This decomposition of the stresses in the ligament, together with the observation that no plastic zones form during fracture, suggest that the fracture process is actually similar to that which would be caused in an unnotched specimen, (W-2c)/2 wide, by the application of nonuniform tension stress σ_T . In particular, one expects that failure will occur when the tension stress in the unbroken fibers ahead of the blunted notch reaches a certain critical magnitude. Therefore, the magnitude of an average stress or strain in a certain representative volume (RV) of the ligament next to the notch may be selected as a fracture criterion.

The above hypothesis was examined by evaluation of the local fields in many center-notched specimens of different dimensions which were tested experimentally. The local fields were evaluated with the finite element method using the ABAQUS program. In its elastic response, the composite was regarded as a homogeneous, transversely isotropic medium; its elastic

constants were selected as equal to self-consistent estimates of the composite moduli. In the plastic range, the constitutive relations of the composite were selected with regard to our recent experimental results [9], and their theoretical interpretation by the bimodal plasticity theory of fibrous composites [10]. Specifically, in the finite element analysis of the notched composites with the ABAQUS program we specified Hill's anisotropic yield condition and adjusted the ellipsoidal yield surface which represents this condition to fit inside the bimodal yield surface.

In addition, the finite element solution was simplified in a manner consistent with our experimental observations for the elastic-plastic behavior of the B-Al composite [9] and the nature of the deformation field observed in notched specimens. In particular, the notched plate was assumed to remain elastic everywhere, except in a narrow band of elements which were designated to represent the plastic shear zone. The band of elements representing the plastic zone was one element wide (0.1mm) and extended from the notch tip in the fiber direction up to the end of the specimen. The rate of hardening in the plastic zone was represented by a bilinear shear stress-plastic shear strain curve given by $\tau/\tau_0 = 1 + 1400 \gamma_P$, for $0 \leq \gamma_P \leq 0.001$; $\tau = \tau^*$, for $\gamma_P \geq 0.001$, where the initial yield stress in shear τ_0 , and τ^* were selected as 40 MPa and 96 MPa, respectively.

The finite element analysis was performed on 17 different specimen geometries selected from our experimental program, and from the program performed at NASA-Langley by Poe and Sova [3]. Space limitations prevent description of most of the results at this time. We present here the principal result of the analysis which appears in Fig. 6. For a total of 39 specimens tested in our program and in the NASA program, the figure shows two computed magnitudes of the normal strain ϵ_{22} in a small representative volume of the composite ahead of the notch tip. The lower shaded band in the figure indicates the magnitudes of the average strains in the ligament, $\epsilon_{lig} = \sigma_{lig}/E_{22}$, caused by the stresses σ_{lig} in Fig. 5. The upper shaded band indicates the total normal strains in a small representative volume of the composite ahead of the notch tip. As the decomposition in Fig. 5 suggests, the total stresses and strains ahead of the notch tip are the sum of the average ligament values and the zone-induced values. Therefore, the zone-induced component of the total strain, $\Delta\epsilon$, in each specimen of Fig. 6, is represented by the strain difference between the respective points in the upper and lower bands. The zone induced contribution to the total strain is the cause of the strength reduction in notched specimens from the net ligament strength, c.f., Figs. 1 and 2.

The total failure strains ϵ_{RV} in Fig. 6 were computed under incremental loading from the unloaded state to the overall level of applied stress equal to experimentally measured fracture strength in each specimen. The dimensions of the representative volume (RV) were selected based on a hexagonal array geometry of the microstructure [11]. For 50% fiber volume fraction, dimension of the RV in the x_1 direction, measured from the notch tip, was selected as 1.55 fiber diameter, which was equal to 220 μm . The strains ϵ_{RV} fall within a narrow band, which suggests that the fracture strength is indeed reached when the local strain attains a critical value. This critical strain value can be approximated by the unnotched failure strain, or found by testing a small number of center-notched specimens and used, together with the present model to predict fracture strength of specimens of other geometries.

5. CONCLUSIONS

The results confirm that the onset of failure in center-notched, unidirectionally reinforced, B-Al specimens is controlled by a critical magnitude of local average strain in a small representative volume of the

composite ahead of the notch tip. They also confirm that the fracture process is not self-similar; long plastic shear zones form at the notch tip before fracture but no such zones appear along the fracture surface.

ACKNOWLEDGEMENTS

This work was supported by the Office of Naval Research.

REFERENCES

1. Awerbuch, J. and Hahn, H.T., "Crack-Tip Damage and Fracture Toughness of Boron/Aluminum Composites," J. Composite Materials, Vol. 13, 1979, pp. 82-107.
2. Jones, W.F., and Goree, J.G., "Fracture Behavior of Unidirectional Boron/Aluminum Composite Laminates," in "Mechanics of Composite Materials 1983", G.J. Dvorak, ed., ASME, AMD-Vol. 58, 1983, pp. 171-177.
3. Poe, C.C., and Sova, J.A., "Fracture Toughness of Boron/Aluminum Laminates With Various Proportions of 0° and ±45° Plies," NASA Technical Paper 1707, 1980.
4. Reedy, E.D., "On the Specimen Dependence of Unidirectional Boron/Aluminum Fracture Toughness," J. of Composite Materials Supplement, Vol. 14, 1980, pp. 118-131.
5. Reedy, E.D., "Notched Unidirectional Boron/Aluminum: Effect of Matrix Properties," J. Composite Materials, Vol. 16, 1982, pp. 495-509.
6. Wright, M.A. and Welch, D., "Failure of Centre Notched Specimens of 6061 Aluminum Reinforced With Unidirectional Boron Fibres," Fibre Science and Technology, Vol. 11, 1978, pp. 447-461.
7. Dharani, L.R., Jones, W.F., and Goree, J.G., "Mathematical Modeling of Damage in Unidirectional Composites," Engineering Fracture Mechanics, Vol. 17, 1983, pp. 555-573.
8. Costin, L.S., Duffy, J., and Freund, L.B., "Fracture Initiation in Metals Under Stress Wave Loading Conditions," in "Fast Fracture and Crack Arrest", G.T. Hahn and M.F. Kanninen, eds., ASTM STP 627, 1977, pp. 301-318.
9. Dvorak, G.J., Bahei-El-Din, Y.A., Macheret, Y., and Liu, C.H., "An Experimental Study of Elastic-Plastic Behavior of a Fibrous Boron-Aluminum Composite," J. Mech. Phys. Solids, in print.
10. Dvorak, G.J., and Bahei-El-Din, Y.A., "A Bimodal Plasticity Theory of Fibrous Composite Materials," Acta Mechanica, Vol. 69, 1987, pp. 219-241.
11. Dvorak, G.J. and Teply, J.L., "Periodic Hexagonal Array Models for Plasticity Analysis of Composite Materials," in Plasticity Today: Modelling, Methods and Applications, W. Olszak Memorial Volume, A. Sawczuk and V. Bianchi, editors, Elsevier, 1985, p. 623.

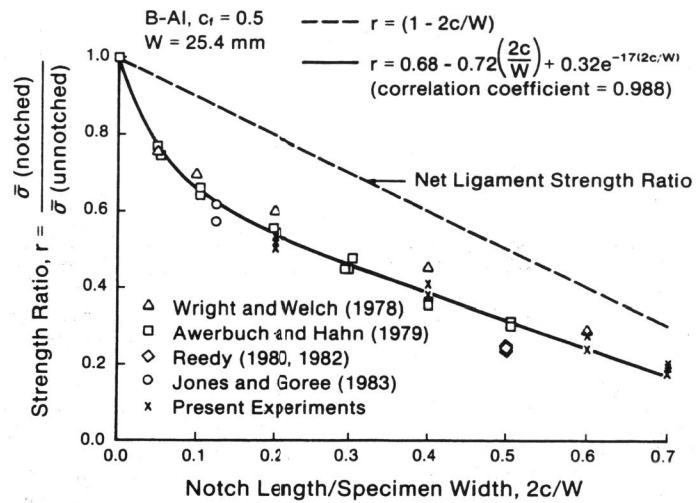


Fig. 1 Experimentally measured relative fracture strength reduction caused by notches in 25.4 mm wide B/Al specimens.

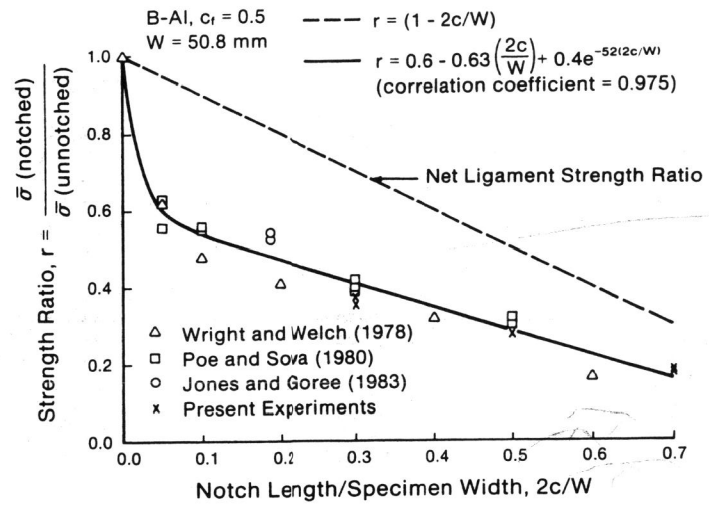


Fig. 2 Experimentally measured relative fracture strength reduction caused by notches in 50.8 mm wide B/Al specimens.

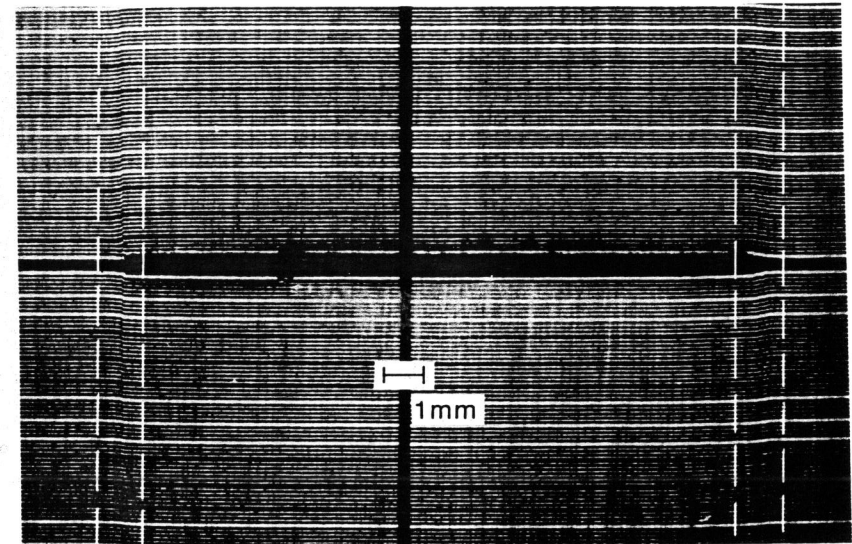


Fig. 3 Distorted parts of the bar code found on specimen B1 at 0.977 of ultimate load. Vertical boundaries were added to enhance visibility.

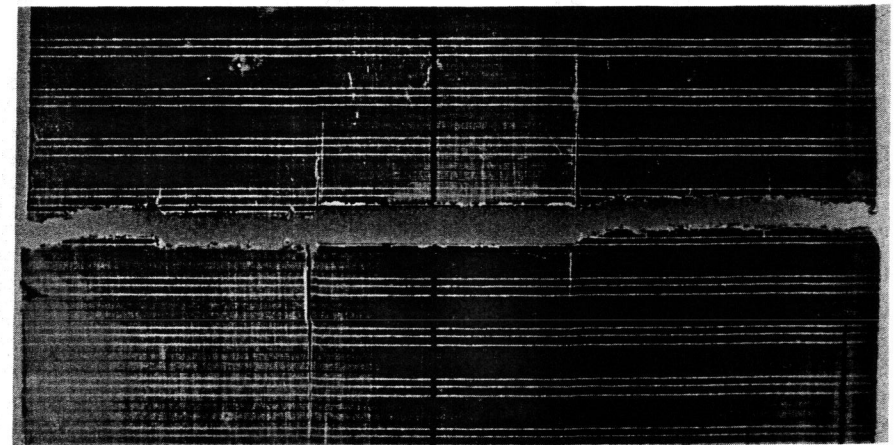


Fig. 4 Photograph of broken specimen B1.

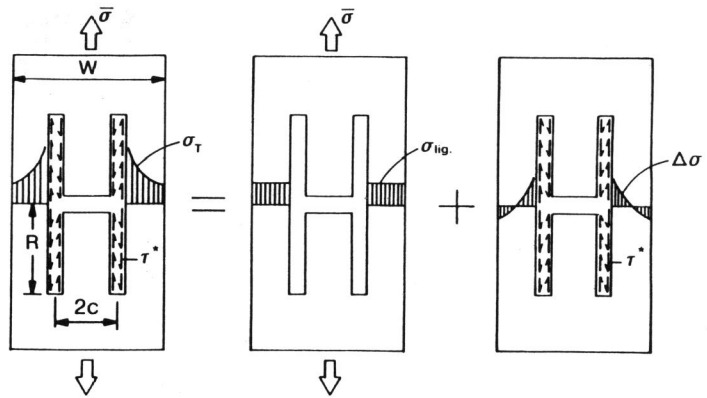


Fig. 5 Schematic decomposition of stress distribution in the ligaments of a center-notched specimen with long plastic zones.

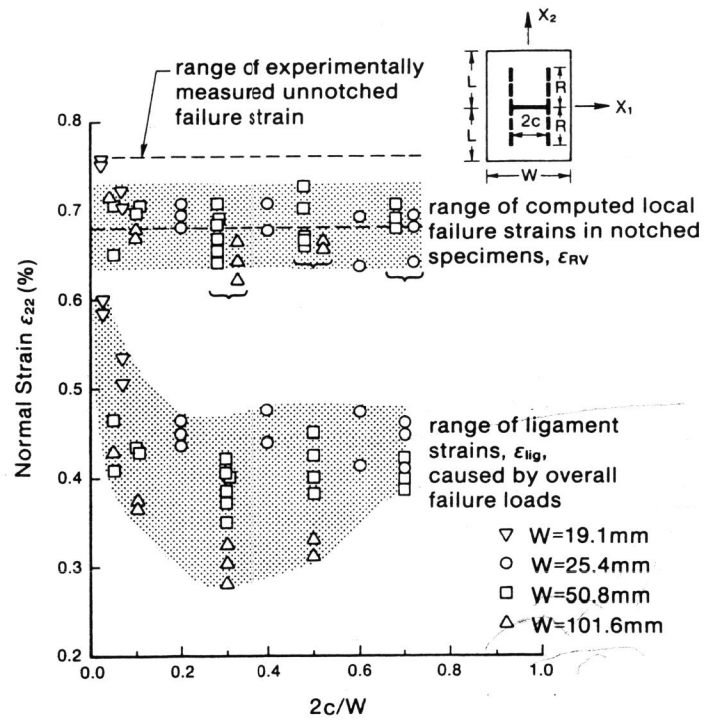


Fig. 6 Computed local failure strains in center-notched B-Al specimens.